Published in final edited form as:
Mol Ther. 2011 April ; 19(4): 642–649. doi:10.1038/mt.2010.293.

Suppression and Replacement Gene Therapy for Autosomal Dominant Disease in a Murine Model of Dominant Retinitis Pigmentosa

Sophia Millington-Ward, PhD[1,*], **Naomi Chadderton, PhD**[1,*], **Mary O'Reilly, PhD**[1], **Arpad Palfi, PhD**[1], **Tobias Goldmann, PhD**[2], **Claire Kilty, BA(Mod)**[1], **Marian Humphries, PhD**[1], **Uwe Wolfrum, PhD**[2], **Jean Bennett, MD/PhD**[3], **Peter Humphries, PhD**[1], **Paul F. Kenna, MD/PhD**[1,§], and **G. Jane Farrar, PhD**[1,§]

[1]Department of Genetics, Smurfit Institute of Genetics, Trinity College Dublin, Dublin 2, Ireland [2]Johannes Gutenberg University of Mainz, Institute of Zoology Cell and Matrix Biology, Muellerweg 6, D-55099 Mainz, Germany [3]F. M. Kirby Center for Molecular Ophthalmology, Scheie Eye Institute, University of Pennsylvania, Philadelphia, Pennsylvania, USA

Abstract

For dominantly inherited disorders development of gene therapies, targeting the primary genetic lesion, has been impeded by mutational heterogeneity. An example is rhodopsin-linked autosomal dominant retinitis pigmentosa with over 150 mutations in the rhodopsin gene. Validation of a mutation-independent suppression and replacement gene therapy for this disorder has been undertaken. The therapy provides a means of correcting the genetic defect in a mutation-independent manner thereby circumventing the mutational diversity. Separate adeno-associated virus vectors were used to deliver an RNA interference-based rhodopsin suppressor and a codon-modified rhodopsin replacement gene resistant to suppression due to nucleotide alterations at degenerate positions over the RNA interference target site. Viruses were subretinally co-injected into *P347S* mice, a model of dominant rhodopsin-linked retinitis pigmentosa. Benefit in retinal function and structure detected by electroretinography and histology, respectively, was observed for at least five months. Notably, the photoreceptor cell layer, absent in five month-old untreated retinas, contained 3-4 layers of nuclei, while photoreceptor ultrastructure, assessed by transmission electron microscopy improved significantly. The study provides compelling evidence that co-delivered suppression and replacement is beneficial, representing a significant step towards the clinic. Additionally dual-vector delivery of combined therapeutics represents an exciting approach, which is potentially applicable to other inherited disorders.

Introduction

It is timely to explore gene therapies for autosomal dominantly inherited rhodopsin-linked retinitis pigmentosa (*RHO*-adRP) given knowledge of the genetic etiology of the disease (1) and data suggesting that recombinant adeno-associated virus (AAV)-mediated subretinal

Correspondence should be addressed to A.P. (palfia@tcd.ie): Department of Where the work was done: Genetics, Smurfit Institute of Genetics, Trinity College Dublin, Dublin 2, Ireland. Phone: +353 1 8962482. Fax: +353 1 8963848..
[*]the first two authors contributed equally to this work.
[§]the last two authors contributed equally to this work.

Conflict of Interest Statement

J.F. and P.K. are directors of Genable Technologies; N.C. A.P. M.O'R. and S.M-W are consultants for Genable Technologies. These authors have conflicting interests.

Europe PMC Funders Author Manuscripts

Europe PMC Funders Author Manuscripts

gene delivery is well tolerated in the human eye (2, 3, 4, 5, 6, 7). *RHO*-adRP leads to the progressive loss of photoreceptors and significant visual dysfunction in 1 in 30,000 people (1, 8, 9). The rhodopsin (*RHO*) gene is extremely highly expressed (10) and constitutes approximately 90% of the total protein content of mammalian rod outer segment (OS) disc membranes. Several modes of action of different *RHO* mutant proteins have been established (11). The disease is immensely heterogeneous with approximately 150 different *RHO* mutations identified thus far (www.sph.uth.tmc.edu/RetNet; www.hgmd.cf.ac.uk).

The mutational heterogeneity present in *RHO*-adRP and many dominant genetic diseases represents a barrier to development of gene-based therapies to correct the primary genetic defect. Therefore, a mutation-independent approach involving two components, RNA interference (RNAi)-based suppression of both mutant and wild type *RHO* alleles and provision of a suppression resistant replacement *RHO* gene (12, 13), is investigated here.

In a previous study of *RHO* suppression and replacement utilizing *P23H* mice, which simulate human *RHO*-adRP, a single dual component AAV vector was evaluated (13). The potential and challenges of the technology were highlighted in the study. While histological benefit in the retina was obtained, functional improvement was not demonstrated; probably due to the extremely rapid nature of the photoreceptor cell degeneration in the *P23H* mouse, where photoreceptor cell loss occurs over approximately a two week period and in addition, to low levels of expression of the replacement *RHO* gene. This promoted optimization and separate evaluation of the RNAi suppression and the replacement components of the therapy. Additionally, these studies were performed in *P347S* mice (another model of *RHO*-adRP where photoreceptor cell loss is much slower given a much larger window of time for therapeutic intervention). RNAi suppression of the mutant *RHO* provided benefit in the presence of the endogenous murine rhodopsin (*Rho*) gene (14). In the study, *Rho*, resistant to suppression due to natural mismatches at the RNAi target site, effectively functioned as a replacement gene.

Given the high expression level of endogenous *Rho* it was apparent that the replacement component of AAV-delivered suppression and replacement required optimization. Therefore a range of *RHO* replacement AAV vectors was generated and evaluated in *Rho*−/− mice (15). Utilization of an optimized rhodopsin promoter, which was far more highly expressed from AAV vectors than earlier constructs, evoked electroretinographic (ERG) responses and resulted in the elaboration of rod OS in *Rho*−/− mice (15).

While generation of an efficacious dual-component gene therapy (encompassing RNAi-based suppression and codon-modified gene replacement) for dominant disease is challenging, demonstration of the efficacy of each component separately stimulated examination of the potential benefit associated with combining the AAV *RHO* suppression and AAV *RHO* replacement therapies. Employing two vectors rather than a single vector enables a further degree of control on relative levels of suppression and replacement. Furthermore, engineering both RNAi-mediated suppression and optimized *RHO* replacement elements into a single AAV vector results in a transgene size at the limit for optimal production of AAV and therefore may result in compromised infectivity, transgene expression and viral titers (16). Hence, in this study we have explored suppression and replacement of *RHO* utilizing co-delivery of the two components of the therapy by two separate AAV vectors and demonstrate the feasibility of this approach in *P347S* mice. The results obtained provide evidence of significant functional benefit and therefore represent a significant step towards the clinic. The proof of concept obtained in this study supports the view that mutation-independent gene-based therapies may be relevant not only for *RHO*-adRP but also for other dominant disorders. Additionally, this dual-vector dual component

approach may be applicable to other gene therapies where AAV packaging size is a limiting factor or a flexible/adaptable control of gene expression is desired.

Results

The focus of this study was to determine whether a suppression and replacement gene therapy involving co-subretinal administration of two AAV vectors, one encoding a *RHO* suppressor (AAV-S) and the other a *RHO* replacement gene (AAV-R), could provide significant benefit in a mouse model of *RHO*-adRP, the *P347S* mouse.

The working hypothesis was that co-administration of two AAVs (AAV-S and AAV-R) would result in co-infection of significant proportions of photoreceptors. In principle these photoreceptors should receive both suppression and replacement components and therefore should function similarly to wild type photoreceptors. To test the feasibility of this approach, co-administration of two AAV vectors each encoding a marker gene was undertaken. Both reporter genes were driven from a *CMV* promoter. A mixture of 1.5×10^9 vp AAV-*EGFP* and 1.5×10^9 vp AAV-*DsRed* was subretinally injected into adult wild type mice and retinas evaluated by histology two weeks later (n=5). Areas of the retinas transduced by the two viruses completely overlapped as determined by microscopic analysis of whole mount retinas (Fig. 1a-c). At the cellular level the majority of the transduced cells co-expressed both markers (yellow) and only a few cells expressed just one marker (red or green; Fig. 1d-f). These experiments provide evidence of significant co-expression following co-administration of two AAVs. The results suggest that a similar strategy using two AAV constructs for delivering the suppression and replacement components should also result in significant co-transduction of photoreceptors.

Initially, 6.0×10^8 vp AAV-S or an AAV expressing a non-targeting control RNAi, AAV-C, were subretinally injected into contralateral eyes of *P347S* mouse pups, which express a human mutant *RHO* transgene. AAV-S has previously been shown to suppress rhodopsin mRNA by greater than 90% *in vivo* (also referred to as siBB, (13)). Two weeks post-injections retinas were harvested, transduced (green) cells collected by FACS and RNA extracted. Levels of mutant *RHO*, determined by quantitative real time RT PCR (qPCR), using human *RHO*-specific primers, were suppressed by 68±2.4% (n=6, p=0.0187) in cells transduced with AAV-S versus AAV-C, indicating that efficient *RHO* suppression has occurred in this disease model of *RHO*-adRP (Fig. 2a). Subsequently the resistance to suppression of transcripts expressed from AAV-R was determined in adult wild type mice. Mixtures of either 6.0×10^8 vp AAV-S and 1.8×10^{10} vp AAV-R or 6.0×10^8 vp AAV-C and 1.8×10^{10} vp AAV-R were subretinally injected into fellow eyes, total RNA extracted two weeks post-injection and RNA analysed. Levels of *RHO* replacement expressed from AAV-R were determined by qPCR and did not differ significantly between the AAV-S and AAV-R or the AAV-C and AAV-R injected eyes (p=0.814, n=7), suggesting that the *RHO* replacement gene delivered in AAV-R is resistant to AAV-S suppression (Fig. 2b). Additionally, subretinal administration of 1.0×10^{10} vp of AAV-R was undertaken in adult wild type mice (n=8) and two weeks post-injection levels of *RHO* expression from AAV-R were compared to levels of expression of *RHO* in normal human rhodopsin (*NHR)* transgenic mice. The *NHR* mouse expresses a wild type human *RHO* transgene at levels comparable with endogenous levels of mouse *Rho* expression and displays a wild type phenotype (17, 13). Comparison of RNA from whole retinas of AAV-R administered to wild type mice and retinas from *NHR* mice demonstrated that *RHO* expression from AAV-R was approximately 31±5% of levels observed in *NHR* mouse retinas. Notably, since only approximately 40% of the retina is thought to be transduced by AAV (Fig. 2c), this suggests that overall expression levels of *RHO* from AAV-R may be similar to endogenous murine *Rho* levels and *RHO* levels in the *NHR* transgenic mouse (Fig. 2c). Quantitative protein

analysis was not undertaken as the human RHO-specific antibody used for immunocytochemistry (see below) is not suitable for Western blotting or ELISA.

In all subsequent experiments five-day old *P347S* mice were subretinally injected. In one set of experiments right eyes were injected with a mixture of 6.0×10^8 vp AAV-S and 1.8×10^{10} vp AAV-R. Fellow left eyes received 6.0×10^8 vp of control AAV-C. As evaluated by six week post-injection ERGs, rod-isolated amplitudes in eyes treated with the mixture of AAV-S and AAV-R were found to be 184.5±65.4 μV compared to fellow eyes treated with control AAV-C, where the amplitudes were 34.9±16.8 μV ($p<0.0001$, n=17; Fig. 3a and c). In twenty week post-injection ERGs, rod-isolated responses were 58.1±19.8 μV in treated eyes compared to 16.9±12.6 μV ($p<0.0001$, n=12) in control eyes (Fig. 3b and c), the latter being similar to that of un-injected eyes (data not shown).

In order to determine if the improved retinal responses resulted from the AAV-S and AAV-R suppression and replacement combination therapy or either component singly, effects of AAV-R and AAV-S were assessed separately. To test the suppression component, 6.0×10^8 vp of AAV-S (right eyes) or control AAV-C (left eyes) were subretinally injected into contralateral eyes. Similarly, to test the replacement component, 1.8×10^{10} vp of AAV-R (right eyes) were subretinally injected while the fellow left eyes remained un-injected. Rod-isolated ERGs, performed six weeks post-injection were not significantly different; 60.5±32.6 μV in AAV-S alone treated eyes compared to 68.1±20.1 μV (n=12) in control eyes, (Figure S1a and c) and 63.7±38.6 μV in AAV-R alone treated eyes compared to 46.4±17.9 μV (n=10) in un-injected eyes (Figure S1b and c) indicating that AAV-S alone or AAV-R alone did not provide benefit in *P347S* mice.

Notably, the benefit observed subsequent to subretinal delivery of the combined suppression and replacement therapy was also observed at the histological level. Six weeks post-injection, outer nuclear layer (ONL) thickness of sections from eyes treated with the mixture of AAV-R and AAV-S was 17.9±3.4 μm compared to 13.3±2.0 μm in sections from control eyes treated with AAV-C ($p<0.0001$, n=5). Preservation of retinal structure was also apparent in semi-thin sections (Figure S2a and b). Transmission electron microscopy (TEM) of these retinas (n=3) demonstrated that only photoreceptor inner segments (IS) were present in control retinas while photoreceptor IS and OS were abundant in AAV-S and AAV-R treated retinas (Figure S2c and d). Due to the presence of OS, the distance between the ONL and the retinal pigment epithelium (RPE) was greater in the treated eyes (Figure S2).

Histological analysis at twenty weeks post-injection demonstrated a striking difference between combined suppression and replacement treated and control eyes. While vestigial ERG responses were still recorded in some control eyes, the ONL had almost completely disappeared (and therefore ONL thickness was not measurable) and rhodopsin protein was not detectable in the control eyes (Fig. 4c and e). In contrast, the ONL in eyes treated with suppression and replacement therapy contained 3-4 layers of photoreceptor nuclei (8.9±1.2 μm thickness; n=4, Fig. 4d and f). Treated retinas were characterized by rhodopsin expression in both the ONL and the photoreceptor segment layer (Fig. 4d and f). Note that EGFP tracer was only present in the RPE of the control eyes (as no photoreceptor layer remained; Fig. 4c) while it was present in both RPE and ONL of the suppression and replacement treated retinas (Fig. 4f). Differences in EGFP intensities between treated and control eyes were apparent in the whole mount retinas (Fig. 4a and b) and were independent of the transduction coverage (approximately 40%). Semi-thin sections demonstrated significant photoreceptor rescue in the treated retinas (Fig. 5a and b). At the ultra-structural level, well-preserved OS characterized the treated retina (Fig. 5d) while only membranous debris was present between the inner nuclear layer (INL) and the RPE (Fig. 5c) in the control retina. High magnification TEM revealed individual photoreceptor segments,

depicted in Fig. 6. Short, degenerating OS with inflated and disorganized membrane disks were present in the control retina at six weeks post-injection (Fig. 6a), while no photoreceptors were found at twenty weeks post-injection. In photoreceptor cells treated with AAV-S and AAV-R, the IS were attached to well preserved OS with parallel layers of tightly stacked membrane disks at both six and twenty weeks post-injection indicating substantial rescue of the photosensitive OS (Fig. 6b and c).

Discussion

The mutational heterogeneity inherent in many autosomal dominantly inherited disorders represents a significant barrier to the development of therapies focused on amending the primary genetic lesion. Suppression and replacement therapies represent a means to circumvent such mutational heterogeneity. In this study the strategy has been explored for *RHO*-adRP. The results obtained clearly demonstrate that RNAi-suppression and codon-modified replacement can be used in concert to provide functional benefit in the *P347S* mouse model of adRP. This should serve to promote the use of the approach for other dominantly inherited conditions such as *RDS*-linked adRP and *COL7A1*-linked Epidermolysis Bullosa amongst others. In this regard a suppression and replacement gene therapy for *SOD-1*-linked autosomal dominantly inherited amyotrophic lateral sclerosis (ALS) has recently been explored in mice (18). RNAi-based suppression and gene replacement of *SOD1* following AAV administration of a single vector was achieved as determined by RNA and protein assays. However, the histological and functional effects of AAV-delivered suppression and replacement were not studied.

Recent clinical trials employing AAV-mediated subretinal delivery of an *RPE65* replacement gene for Leber Congenital Amaurosis (LCA) have suggested that AAV is well tolerated in the human eye and have promoted the use of AAV for retinal gene delivery (2, 3, 4, 5, 6, 7). In addition, an inverse relationship between age of treatment and level of benefit was observed (5). Given the encouraging result from the LCA clinical trials, AAV (2/5) was adopted in the current study as the virus of choice to administer suppression and replacement therapies to *P347S* mice.

While the clinical applications of AAV make it an attractive choice for gene delivery to the retina, transgene size constraints associated with AAV promoted the exploration of viral mixtures consisting of two separate AAV suppression and replacement vectors. Using reporter viruses (AAV-*EGFP* and AAV-*DsRed*) initially, it was established that a substantial photoreceptor co-infection with the two vector after a single subretinal injection of vector mixtures (Fig. 1 a-f). This encouraged the subsequent assessment of therapeutic co-administration of AAV-S and AAV-R in *P347S* mice. Of note, the dual vector strategy also allows a further level of control on the relative *RHO* suppression and replacement levels. To limit the probability of *RHO* suppression in the absence of *RHO* replacement, a greater amount of the AAV-R vector was employed. The dose of AAV-R chosen was the maximum possible given the AAV-R viral titer and one that had been previously shown to provide structural and functional benefit in the *Rho*−/− mouse (15). The dose of AAV-S used was the minimum required to achieve high levels of suppression (14). With regard to transgene size, there have been reports of transgenes of approximately 9kb in AAV2/5 vectors (19). However potential effects on titer and transgene expression remain unresolved (16). Three groups have since independently attempted to repeat packaging of large cassettes (20, 21, 22) but their studies to date indicate that the packaging capacity of AAV is usually limited to about 5 kb. Hence a dual vector approach for suppression and replacement was adopted in the current study.

Europe PMC Funders Author Manuscripts

Subretinal injections were undertaken at P5 in *P347S* mice to enable early administration of the gene therapy while minimising surgical trauma that had previously been observed in younger animals, for example, in P0 and P1 injected eyes (data not shown). Significant and consistent evidence of therapeutic benefit was obtained using both electrophysical and histological readouts. ERG comparisons between treated and control eyes at 6 weeks and 5 months demonstrated significantly improved responses in AAV-S and AAV-R dual-treated eyes (Fig. 3a-c). The beneficial effects observed using ERG were also observed using histological analyses employing both light and electron microscopy. Retention of ONL (3-4 rows) was observed in treated *P347S* eyes 5 months subsequent to a single subretinal injection of AAV-S and AAV-R, whereas in contrast, there were no remaining rows of photoreceptor nuclei in the ONL of control eyes (Fig. 4). Likewise, improved photoreceptor OS ultrastucture was detected by TEM in treated versus control *P347S* mouse eyes (Figs. 5 and 6).

While the AAV-S and AAV-R combination therapy was found to provide functional benefit in *P347S* mouse eyes when compared to control eyes, it was important to establish if either of these components alone provided the beneficial effect. Subretinal injection of AAV-S alone or AAV-R alone (using the same vector doses as employed in the AAV-S and AAV-R combination therapy) did not provide significant therapeutic benefit in *P347S* mice when treated and control eyes were compared (Figure S1a-c). Note that the relatively low dose of AAV-S used resulted in a modest but not significant reduction in ERG in the AAV-S treated eyes compared to eyes treated with AAV-C. In contrast ERG responses in AAV-R alone treated eyes were slightly enhanced when compared to control eyes but this difference did not reach statistical significance. Indeed it was the combination of AAV-mediated suppression in conjunction with AAV-mediated replacement that was required to obtain benefit in this mouse model of *RHO*-adRP. It is worth noting that while the use of two separate AAV vectors for gene delivery is of direct relevance for suppression and replacement therapies where two components are essential, employing a dual-vector approach may also be of value where delivery of two synergistic therapies could potentially augment benefit. One example may be the delivery of a gene replacement therapy together with a neurotrophic factor for some autosomal recessively inherited disorders (23) amongst other combinations. Undoubtedly the use of dual-vectors will be explored more extensively in the future in an attempt to optimize gene-based therapeutics for many disorders. The results from the current study validate the principle of a two-vector approach.

Suppression and replacement provides a means of correcting the primary genetic defect and will be particularly relevant where the mutant protein drives the disease process. Alternative therapeutic approaches focused on modulating secondary effects associated with the disease are also being contemplated for adRP; many of these are focused on modulating secondary effects associated with the disease. Some of these strategies have been evaluated in rodent models of adRP and beneficial effects of the therapy observed. Such approaches include provision of neurotrophic factors and / or anti-apoptotic factors, modulation of oxidative stress, cell replacement strategies and reduction of protein aggregates (24, 25, 26, 27, 28). Typically these approaches are being evaluated not solely for retinal degenerations but a broad range of neurodegenerative conditions. Indeed at times multivalent therapies involving a combination of strategies may be required to protect photoreceptors from degeneration precipitated by the presence of dominant mutations. The modes of action of different dominant *RHO* mutations can vary significantly and for some *RHO* mutations remain undetermined. These mechanisms may involve, for example, incorrect rhodopsin transport to the outer segments, rhodopsin misfolding or may affect endocytosis or protein stability (11). In principle, *RHO* suppression and replacement is relevant to *RHO*-linked adRP patients irrespective of the mode of action of a particular *RHO* mutation.

The potential power of viral vector-mediated RNA interference as a therapeutic tool has been reviewed (29). In the current study, a strategy to correct the primary genetic defect in *RHO*-linked adRP was evaluated using two AAV viruses to deliver a dual component therapy. RNAi-mediated suppression of *RHO* in conjunction with provision of an RNAi-resistant *RHO* replacement gene engineered using codon redundancy was found to provide functional benefit in the *P347S* mouse. This represents the first demonstration for any dominant condition that an AAV-delivered dual component therapy (involving gene suppression and replacement) targeted at amending the primary defect can provide functional benefit. Employing RNAi in concert with replacement genes exploiting codon redundancy provides a means to overcome the mutational diversity asssociated with many autosomal dominant conditions. The results obtained provide the impetus to progress this therapeutic approach for *RHO*-adRP towards clinical trial.

Materials and Methods

Vector Construction and AAV Production

RHO-targeting RNAi (*shBB*; target position nt 254-274, accession no. NM_000539.2 and non-targeting control RNAi (*shNT*; 5-TTCTCCCAACGAGTCACGTTTCAAGAGAACGTGACACGTTCGGAGAATTTTT-3) were cloned into pAAV-MCS (Stratagene) as described (14). shNT was guaranteed by the manufacturere (Qiagen) not to target any human or murine RNA sequences. shNT has previously been compared to other non-targeting control shRNAs and was shown to be equivalent (data not shown. A *CMV* promoter (*CMV*-P) including the *CMV* enhancer (*CMVE*; Accession No: EF550208) and the SV40 polyadenylation were used in both shRNA constructs to drive expression of an *EGFP* reporter gene (Accession No: U57608; Clontech), creating pAAV-S (*shBB-EGFP*) and pAAV-C (*shNT-EGFP*). Replacement human *RHO* cDNA sequence was constructed by modifying the wild type human *RHO* sequence (Accession No: NM_000539.2) at nt 254–274 as follows 5′-ATAAATTTTTTGACCCTGTAT-3′ (altered bases underlined, 13). Replacement *RHO* (pAAV-R) was driven by a hybrid murine *Rho* promoter originally described as pAAV-*BB24* (15), which contains a 1.7kb mouse rhodopsin promoter (Rho-P) together with two conserved *Rho*-P elements (element E, accession no. NT_005612, nt 35742513-35742578 and element B, accession number AC142099.3, nt 24955-24880), a 0.4kb fragment of the endogenous 3′-UTR, and a minimal polyadenylation signal (30). The *EGFP* (Accession No: U57608; Clontech) and *DsRed-Express2* genes (*DsRed*; accession no. FJ226077; Clontech) driven by a *CMV* promoter were also cloned into pAAV-MCS.

Constructs were packaged into helper-free recombinant AAV2/5 viruses (AAV) as described, (13) to generate AAV-*shBB-EGFP* (AAV-S), AAV-*shNT-EGFP* (AAV-C), AAV-*BB24* (AAV-R), AAV-*EGFP* and AAV-*DsRed*. Briefly, the expression cassettes were transfected into human embryonic kidney (HEK)-293 cells (ATCC [accession number CRL-1573]) with pRep2/Cap5 (31) and pHelper (Stratagene). Fifty 150-mm plates of confluent cells were transfected using polyethylenimine. Forty-eight hours post-transfection, crude viral lysates were cleared and purified by cesium-gradient centrifugation. AAV-containing fractions were dialysed against PBS. Genomic titers (viral particles per ml; vp/ml) were determined by qPCR (32).

Animals and Subretinal Injections

Mutant transgenic *RHO*-Pro347Ser+/− *Rho+/−,* (P347S; 33, 34, 14) and wild type mice were used in this study. All animals were on a 129 S2/SvHsd (Harlan, UK) background. Mice were maintained under specific pathogen free (spf) housing conditions. Sub-retinal injections were carried out in strict compliance with the European Communities Regulations

2002 and 2005 (Cruelty to Animals Act) and the Association for Research in Vision and Ophthalmology (ARVO) statement for the use of animals as described (13). Briefly, adult mice were anesthetized by intraperitoneal injection of medetomidine and ketamine (10 and 750 mg/10 g body weight, respectively). Pupils were dilated with 1% cyclopentolate and 2.5% phenylephrine, and, using topical anaesthesia (Amethocaine), a small puncture was made in the sclera. A 34-gauge blunt-ended microneedle attached to a 10 μl-Hamilton syringe was inserted through the puncture, and AAV was administered to the subretinal space. Following subretinal injection, an anesthetic reversing agent (100 mg/10 g body weight; Atipamezole Hydrochloride) was delivered by intraperitoneal injection. Body temperature was maintained using a homeothermic heating device. Five day-old mice were prepared for subretinal injection as described (35). Adult and five day-old mice were injected with 3 μl and 0.6 μl AAV, respectively. Typically between five and seven adult mice were used per group in order to obtain significance. However, between ten and seventeen five day-old mice per group were used, due to greater injection variability associated with small eye sizes. All animal studies have been approved by the authors' Institutional Review Board.

RNA extraction and qPCR analysis

Adult *P347S* mice (n=6) were subretinally injected with 6.0×10^8 vp AAV-S while fellow eyes received 6.0×10^8 vp AAV-C. Retinas were harvested two weeks post-injection, transduced (green) cells collected by FACS and RNA extracted from these cells (14). Levels of mutant *RHO* expression were determined by qPCR using human *RHO*-specific primers previously described (13). Adult wild type mice were subretinally injected with mixtures of 6.0×10^8 vp AAV-S and 1.8×10^{10} vp AAV-R (n=7) or 6.0×10^8 vp AAV-C and 1.8×10^{10} vp AAV-R (n=7). Two weeks post-injection eyes were harvested, RNA extracted from whole retinas and qPCRs, using human *RHO*-specific primers, performed to determine levels of replacement *RHO* expression as described (13). Adult wild type mice were subretinally injected with 1.0×10^{10} vp of AAV-R (n=8). Two weeks post-injection retinas were collected, total RNA extracted and levels of replacement *RHO* expression compared to levels of *RHO* mRNA in *NHR* mouse retinas by qPCR using human *RHO*-specific primers (13).

Electroretinography (ERG)

ERG procedures have been described in detail (13, 14). Briefly, intraperitoneal administration of Ketamine and Xylazine (16 and 1.6 mg/10g body weight, respectively) were used for anesthesia. Pupils were dilated with 1% Cyclopentalate and 2.5% Phenylephrine and eyes were maintained in a proptosed position throughout the examination. Reference and ground electrodes were positioned subcutaneously, approximately 1 mm from the temporal canthus and anterior to the tail respectively. The ERG responses were recorded simultaneously from both eyes using goldwire electrodes (Roland Consult Gmbh); these were positioned to touch the central cornea of each eye. Corneal hydration and electrical contact were maintained by the application of Vidisic (Dr. Mann Pharma, Berlin, Germany) to the cornea. Standardized flashes of light were presented to the mouse in a Ganzfeld bowl. Responses were analysed using a RetiScan RetiPort electrophysiology unit (Roland Consulting Gmbh). The protocol used was based on that approved by the International Clinical Standards Committee for human ERG. Rod-isolated responses were recorded using a dim white flash (−25 dB maximal intensity where maximal flash intensity was 3 candelas/m^2/s) presented in the dark-adapted state. The a-waves were measured from the baseline to the trough and b-waves from the baseline (standard convention). Following ten minutes light adaptation (30 candelas/m^2) cone responses were recorded to the standard flash presented at 0.5 Hz and 10 Hz flicker against the rod suppressing background.

Microscopy and Statistical Analysis

Rhodopsin immunocytochemistry and fluorescence microscopy were performed as described (13). For immunocytochemistry, the primary rhodopsin antibody was used in 1:100 dilution (courtesy of R. Molday). Outer nuclear layer (ONL) thickness was measured in AAV transduced parts of the retina. Measurements were made at three points per section and three sections per retina. The sections were approximately 100 mm apart and within 300 mm of the optic nerve head. Measurements were made using the ruler tool in Photoshop (Adobe Systems Europe, Glasgow, UK). Procedures for transmission electron microscopy were previously described (36, 15). Briefly, for tissue preparation eyes were enucleated, fixed in 4% paraformaldehyde in PBS, and whole mounted. Using the EGFP tracer, EGFP-positive areas from the central part of the retinas were excised and fixed in 2.5% glutaraldehyde in 0.1 M Cacodylate buffer (pH 7.3) for 2 hrs at room temperature. Specimens were washed and fixed in buffered 2% osmium tetroxide, dehydrated and embedded in Araldite. Semi- and ultra-thin sections were cut and ultrastructural analyses were performed using a Tecnai 12 BioTwin transmission electron microscope (FEI, Eindhoven, NL).

Statistical Analysis

Means and standard deviation values (SD) of ERG, mRNA and histology data sets were calculated. Student's *t*-Tests were used to determine statistical significance between corresponding data sets. Paired *t*-Tests were applied to ERG data. In addition, Wilcoxon Signed Rank tests were undertaken on mRNA and histology data sets and Paired Sign tests on ERG data sets to establish that statistical significance was maintained using non-parametric statistical models. Differences of $p<0.05$ were considered statistically significant.

Supplementary Material

Refer to Web version on PubMed Central for supplementary material.

Acknowledgments

We thank Prof. Wolfgang Baehr (University of Utah, Salt Lake City, UT) for the original *RHO* cDNA construct, Prof. Tiensen Li for the *P347S* mouse (Harvard Medical School, Boston, MA), Elisabeth Sehn (Johannes Gutenberg University, Mainz, Germany) for skillful technical assistance, Prof. Robert S. Molday (University of British Colombia, Vancouver BC, CA) for the rhodopsin primary antibody and the staff of the Bioresources Unit, Trinity College Dublin. The research was supported by grant awards from Science Foundation Ireland, Fighting Blindness Ireland, Foundation Fighting Blindness-National Neurovision Research Institute (USA), Enterprise Ireland, I.R.C.S.E.T. "The embark initiative", EviGenoRet (LSHG-CT-2005-512036), Deutsche Forschungsgemeinschaft (GRK1044), FAUN-Stiftung.

References

1. Farrar GJ, Palfi A, Kenna PF, O'Reilly M. Gene therapeutic approaches for dominant retinopathies. Curr Gene Ther. 2010; 10:381–388. [PubMed: 20712579]
2. Bainbridge JW, Smith AJ, Barker SS, Robbie S, Henderson R, Balaggan K, et al. Effect of gene therapy on visual function in Leber's congenital amaurosis. N Engl J Med. 2008; 358:2231–2239. [PubMed: 18441371]
3. Hauswirth WW, Aleman TS, Kaushal S, Cideciyan AV, Schwartz SB, Wang L, et al. Treatment of Leber congenital amaurosis due to RPE65 mutations by ocular subretinal injection of adeno-associated virus. Hum Gene Ther. 2008; 19:979–990. [PubMed: 18774912]
4. Maguire AM, Simonelli F, Pierce EA, Pugh EN Jr, Mingozzi F, Bennicelli J, et al. Safety and efficacy of gene transfer for Leber's congenital amaurosis. N Engl J Med. 2008; 358:2240–2248. [PubMed: 18441370]

5. Maguire AM, High KA, Auricchio A, Wright JF, Pierce EA, Testa F, et al. Age-dependent effects of RPE65 gene therapy for Leber's congenital amaurosis: a phase 1 dose-escalation trial. Lancet. 2009; 374:1597–1605. 2009. Erratum in: Lancet 2009; 375: 30. [PubMed: 19854499]
6. Simonelli F, Maguire AM, Testa F, Pierce EA, Mingozzi F, Bennicelli JL, et al. Gene therapy for Leber's congenital amaurosis is safe and effective through 1.5 years after vector administration. Mol Ther. 2010; 18:643–650. [PubMed: 19953081]
7. Koenekoop RK. Successful *RPE65* gene replacement and improved visual function in humans. Ophthalmic Genet. 2008; 29:89–91. [PubMed: 18766986]
8. Farrar GJ, Kenna PF, Humphries P. On the genetics of retinitis pigmentosa and on mutation-independent approaches to therapeutic intervention. EMBO JOURNAL. 2002; 21:857–864. [PubMed: 11867514]
9. Wright AF, Chakarova CF, Abd El-Aziz MM, Bhattacharya SS. Photoreceptor degeneration: genetic and mechanistic dissection of a complex trait. Nat Rev Genet. 2010; 11:273–284. [PubMed: 20212494]
10. Palczewski K, Hofmann KP, Baehr W. Rhodopsin—Advances and perspectives. Vision Res. 2006; 46:4425–4426. [PubMed: 17098052]
11. Mendes HF, van der Spuy J, Chapple JP, Cheetham ME. Mechanisms of cell death in rhodopsin retinitis pigmentosa; implications for therapy. Trends Mol Med. 2005; 11:177–185. [PubMed: 15823756]
12. Millington-Ward S, O'Neill B, Tuohy G, Al-Jandal N, Kiang AS, Kenna PF, et al. Strategems *in vitro* for gene therapies directed to dominant mutations. Hum Mol Genet. 1997; 6:1415–1426. [PubMed: 9285777]
13. O'Reilly M, Palfi A, Chadderton N, Millington-Ward S, Ader M, Cronin T, et al. RNA interference-mediated suppression and replacement of human rhodopsin *in vivo*. Am J Hum Genet. 2007; 81:127–135. 2007. [PubMed: 17564969]
14. Chadderton N, Millington-Ward S, Palfi A, O'Reilly M, Tuohy G, Humphries MM, et al. Improved retinal function in a mouse model of dominant retinitis pigmentosa following AAV-delivered gene therapy. Mol Ther. 2009; 17:593–599. [PubMed: 19174761]
15. Palfi A, Millington-Ward S, Chadderton N, O'Reilly M, Goldmann T, Humphries MM, et al. Adeno-associated virus-mediated rhodopsin replacement provides therapeutic benefit in mice with a targeted disruption of the rhodopsin gene. Hum Gene Ther. 2010; 21:311–323. [PubMed: 19824806]
16. Hirsch ML, Agbandje-McKenna M, Samulski RJ. Little vector, big gene transduction: fragmented genome reassembly of□ adeno-associated virus. Mol Ther. 2010; 18:6–8. [PubMed: 20048740]
17. Olsson JE, Gordon JW, Pawlyk BS, Roof D, Hayes A, Molday RS, et al. Transgenic mice with a rhodopsin mutation (Pro23His): a mouse model of autosomal dominant retinitis pigmentosa. Neuron. 1992; 9:815–830. [PubMed: 1418997]
18. Kubodera T, Yamada H, Anzai M, Ohira S, Yokota S, Hirai Y, et al. *In vivo* application of an RNAi strategy for the selective suppression of a mutant allele. Hum Gene Ther. 2010 epub ahead of print 22 July 2010; doi:10.1089/hum.2010.054.
19. Allocca M, Doria M, Petrillo M, Colella P, Garcia-Hoyos M, Gibbs D, et al. Serotype-dependent packaging of large genes in adeno-associated viral vectors results in effective gene delivery in mice. J Clin Invest. 2008; 118:1955–1964. [PubMed: 18414684]
20. Dong B, Nakai H, Xiao W. Characterization of genome integrity for oversized recombinant AAV vector. Mol Ther. 2010; 18:87–92. [PubMed: 19904236]
21. Lai Y, Yue Y, Duan D. Evidence for the failure of adeno-associated virus serotype 5 to package a viral genome > or = 8.2kb. Mol Ther. 2010; 18:75–79. [PubMed: 19904238]
22. Wu Z, Yang H, Colosi P. Effect of Genome Size on AAV Vector Packaging. Mol Ther. 2010; 18:80–86. [PubMed: 19904234]
23. Buch PK, Mac Laren RE, Duran Y, Balaggan KS, MacNeil A, Schlichtenbrede F, et al. In contrast to AAV-mediated Cntf expression, AAV-mediated Gdnf expression enhances gene replacement therapy in rodent models of retinal degeneration. Mol Ther. 2006; 14:700–709. [PubMed: 16872907]

24. Gorbatyuk MS, Knox T, LaVail MM, Gorbatyuk OS, Noorwez SM, Hauswirth WW, et al. Restoration of visual function in P23H rhodopsin transgenic rats by gene delivery of BiP/Grp78. Proc Natl Acad Sci U S A. 2010; 107:5961–5966. [PubMed: 20231467]
25. Tam LC, Kiang AS, Campbell M, Keaney J, Farrar GJ, Humphries MM, et al. Prevention of autosomal dominant retinitis pigmentosa by systemic drug therapy targeting heat shock protein 90 (Hsp90). Hum Mol Genet. 2010 epub ahead of print. 20 September 2010; doi:10.1093/hmg/ddq369.
26. Gregory-Evans K, Chang F, Hodges MD, Gregory-Evans CY. Ex vivo gene therapy using intravitreal injection of GDNF-secreting mouse embryonic stem cells in a rat model of retinal degeneration. Mol Vis. 2009; 15:962–973. [PubMed: 19461934]
27. Yang Y, Mohand-Said S, Danan A, Simonutti M, Fontaine V, Clerin E, et al. Functional cone rescue by RdCVF protein in a dominant model of retinitis pigmentosa. Mol Ther. 2009; 17:787–795. [PubMed: 19277021]
28. Samardzija M, Wenzel A, Thiersch M, Frigg R, Remé C, Grimm C. Caspase-1 ablation protects photoreceptors in a model of autosomal dominant retinitis pigmentosa. Invest Ophthalmol Vis Sci. 2006; 47:5181–5190. [PubMed: 17122101]
29. Couto LB, High KA. Viral vector-mediated RNA interference. Curr Opin Pharm. 2010; 10:1–9.
30. Levitt N, Briggs D, Gil A, Proudfoot NJ. Definition of an efficient synthetic poly(A) site. Genes Dev. 1989; 3:1019–1025. [PubMed: 2570734]
31. Hildinger M, Auricchio A, Gao G, Wang L, Chirmule N, Wilson JM. Hybrid vectors based on adeno-associated virus serotypes 2 and 5 for muscle-directed gene transfer. J Virol. 2001; 75:6199–6203. [PubMed: 11390622]
32. Rohr UP, Wulf MA, Stahn S, Steidl U, Haas R, Kronenwett R. Fast and reliable titration of recombinant adeno-associated virus type 2 using quantitative real-time PCR. J Virol Methods. 2002; 106:81–88. [PubMed: 12367732]
33. Li T, Snyder WK, Olsson JE, Dryja TP. Transgenic mice carrying the dominant rhodopsin mutation P347S: evidence for defective vectorial transport of rhodopsin to the outer segments. Proc Natl Acad Sci U S A. 1996; 93:14176–14181. [PubMed: 8943080]
34. Humphries MM, Rancourt D, Farrar GJ, Kenna P, Hazel M, Bush RA, et al. Retinopathy induced in mice by targeted disruption of the rhodopsin gene. Nat Genet. 1997; 15:216–219. [PubMed: 9020854]
35. Matsuda T, Cepko CL. Electroporation and RNA interference in the rodent retina *in vivo* and *in vitro*. Proc Natl Acad Sci USA. 2004; 101:16–22. [PubMed: 14603031]
36. Wolfrum U. Cytoskeletal elements in arthropod sensilla and mammalian photoreceptors. Biol Cell. 1992; 76:373–381. [PubMed: 1305480]

Europe PMC Funders Author Manuscripts

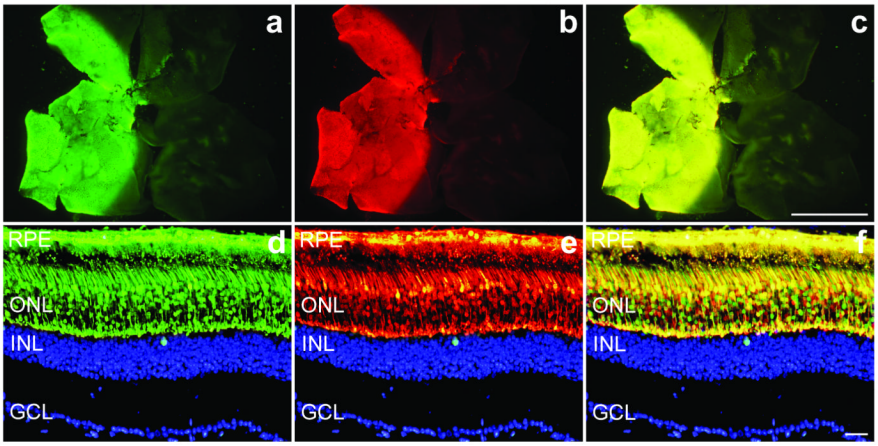

Figure 1.

Co-transduction of AAVs in wild type retinas.

Eyes of wild type mice were subretinally injected with a mixture of 1.5×10^9 vp AAV-*EGFP* and 1.5×10^9 vp AAV-*DsRed*. Two weeks post-injection eyes were fixed (n=5), whole mounted for imaging, then cryosectioned (12 μm) and processed for histology. Nuclei were counterstained with DAPI. a, b and c: representative whole mounts illustrating EGFP (a), DsRed (b) and overlay of EGFP and DsRed signals (c). Representative sections demonstrate significant co-expression (f) of EGFP (d) and DsRed (e) signals at the cellular level in the outer nuclear layer. In order to obtain a clearer view of the markers the DAPI (blue) signal was edited out from the ONL. RPE: retinal pigment epithelium; ONL: outer nuclear layer; INL: inner nuclear layer; GCL: ganglion cell layer. Scale bars: 1 mm (a, b and c) and 25 μm (d, e and f).

Europe PMC Funders Author Manuscripts

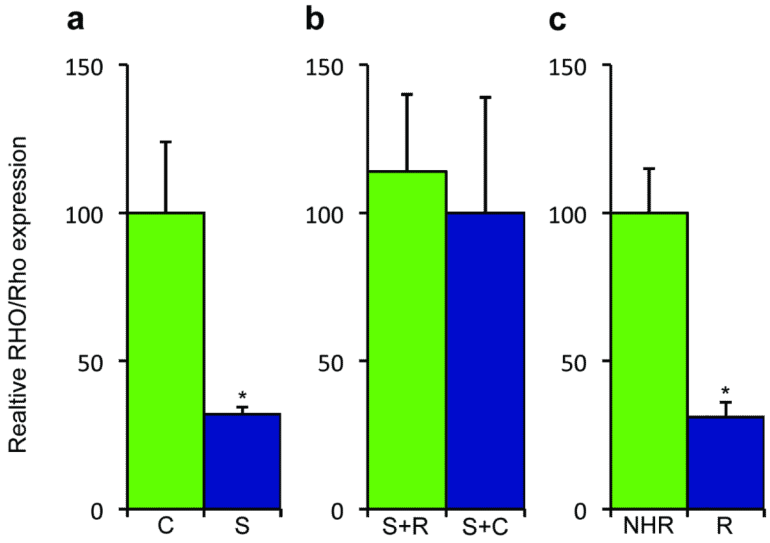

Figure 2.

Rhodopsin mRNA expression levels.

a. Contralateral eyes of adult *P347S* mice (n=6) expressing a mutant human *RHO* transgene were subretinally injected with 6.0×10^{8} vp AAV-S or AAV-R. Two weeks post-injection retinas were harvested, transduced (green) cells collected by FACS and RNA extracted. The level of human *RHO* suppression by AAV-S, determined by qPCR using human-specific *RHO* primers, was 68±2.4%. b. Adult wild type mice (n=7) were subretinally injected with a mixture of either 6.0×10^{8} vp AAV-S and 1.8×10^{10} vp AAV-R or 6.0×10^{8} vp AAV-C and 1.8×10^{10} vp AAV-R. Two weeks post-injection total RNA was extracted and levels of replacement *RHO* RNA determined by qPCR. No significant difference in replacement transcript levels was observed in eyes that received AAV-R and AAV-S versus AAV-R and AAV-C, indicating that no significant suppression of the replacement transcript had occurred (p=0.814). c. Adult wild type mice (n=8) were subretinally injected with AAV-R. Total RNA was extracted two weeks post-injection and levels of *RHO* replacement expression from AAV-R compared to levels of *RHO* in *NHR* mouse retinas. Levels of *RHO* mRNA expression from the AAV-R was 31±5% of levels in *NHR* mouse retinas.

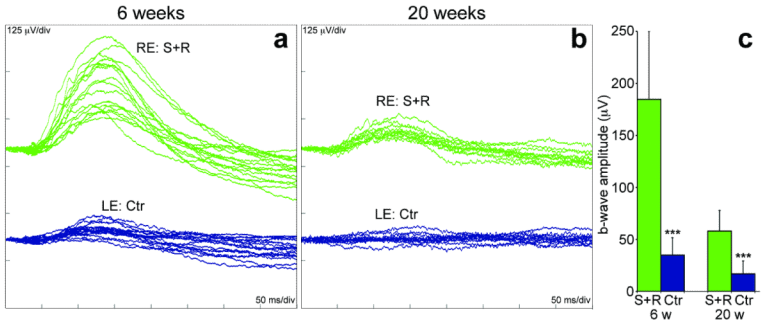

Figure 3.

Rod-derived ERG following combined suppression and replacement therapy.

The right eyes of P5 *P347S* mice were subretinally injected with a mixture of 6.0×10^{8} vp AAV-S and 1.8×10^{10} vp AAV-R while the left eyes were injected with 6.0×10^{8} vp AAV-C. Six (n=17) or twenty weeks (n=12) post-injection, mice were dark-adapted overnight and rod-isolated ERG responses recorded from both eyes. a and b: overlays of the ERG recordings; green and blue lines represent recordings from combined suppression and replacement therapy (S+R) and control (C)-injected eyes, respectively. c: mean ERG b-wave amplitudes (μV). Green and blue columns represent values corresponding to S+R and control injected eyes, respectively. Error bars represent SD values and *** represent $p<0.001$.

Europe PMC Funders Author Manuscripts

Europe PMC Funders Author Manuscripts

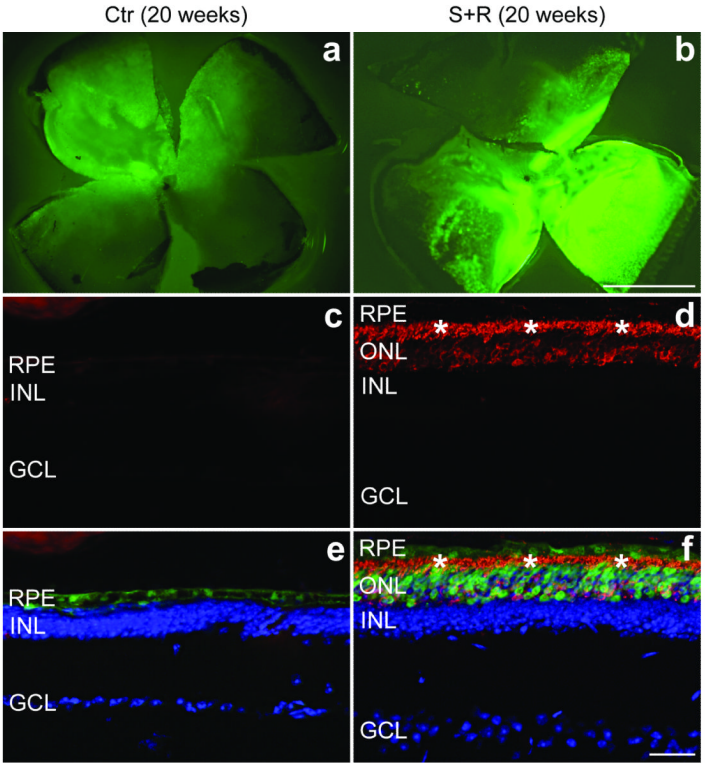

Figure 4.

Immunohistochemical analysis of rhodopsin expression following combined suppression and replacement therapy twenty weeks post-injection.

The right eyes of P5 *P347S* mice were subretinally injected with a mixture of 6.0×10^{8} vp AAV-S (b, d and f) and 1.8×10^{10} vp AAV-R while the left eyes were injected with 6.0×10^{8} vp AAV-C (a, c and e). Note that AAV-S and AAV-C co-express EGFP. Eyes were fixed (n=5), whole mounted for imaging, then cryosectioned (12 μm) and processed for immunocytochemistry using rhodopsin primary and Cy3-conjugated secondary antibodies. Nuclei were counterstained with DAPI. a and b: representative whole mounts. c and d: representative sections show rhodopsin labelling (red). e and f: rhodopsin (red), EGFP (green) and nuclear DAPI (blue) signals overlaid. *: photoreceptor segment layer; ONL: outer nuclear layer; INL: inner nuclear layer; GCL: ganglion cell layer; RPE: retinal pigment epithelium. Scale bars: 1 mm (a and b) and 25 μm (c–f).

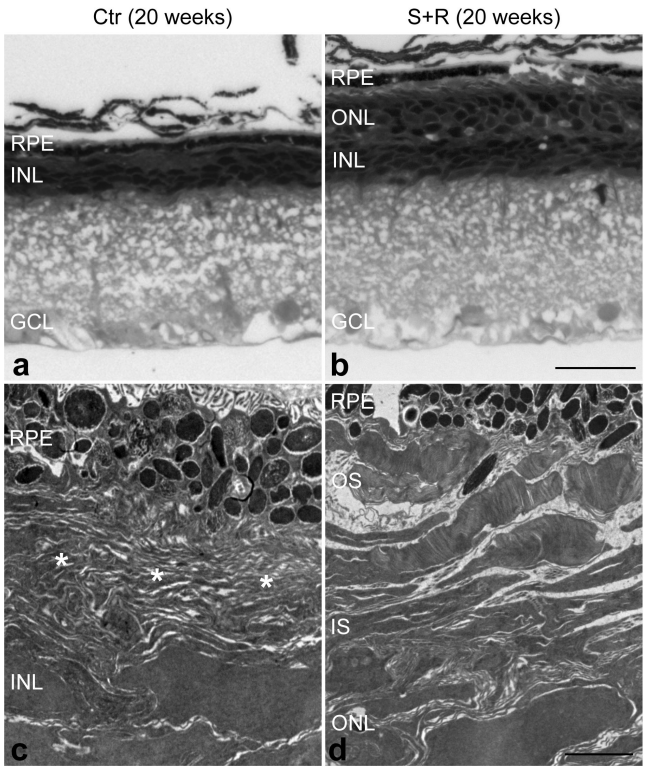

Figure 5.

Ultra-structural analysis of combined suppression and replacement treated retinas twenty weeks post-injection.

The right eyes of P5 *P347S* mice were subretinally injected with a mixture of 6.0×10^{8} vp AAV-S and 1.8×10^{10} vp AAV-R (b and d) while the left eyes were injected with 6.0×10^{8} vp AAV-C (a and c). Note that AAV-S and AAV-C co-express EGFP. Eyes were fixed, whole mounted, and transduced areas identified by EGFP fluorescence and excised. The excised retinal samples were post-fixed and processed for transmission electron microscopy (TEM). Semi- and ultra-thin sections were analysed by light microscopy (a and b) or TEM (c and d). Combined suppression and replacement therapy resulted in preservation of rod photoreceptor outer segments (OS), which extended to the retinal pigment epithelium (RPE; b and d). In contrast, in the control retina, only membranous debris (*) was detected between the RPE and the inner nuclear layer (INL) while the outer nuclear layer (ONL) was not present (a and c). IS: inner segment layer, GCL: ganglion cell layer. Scale bars: 25 μm (a and b) and 2 μm (c and d).

Europe PMC Funders Author Manuscripts

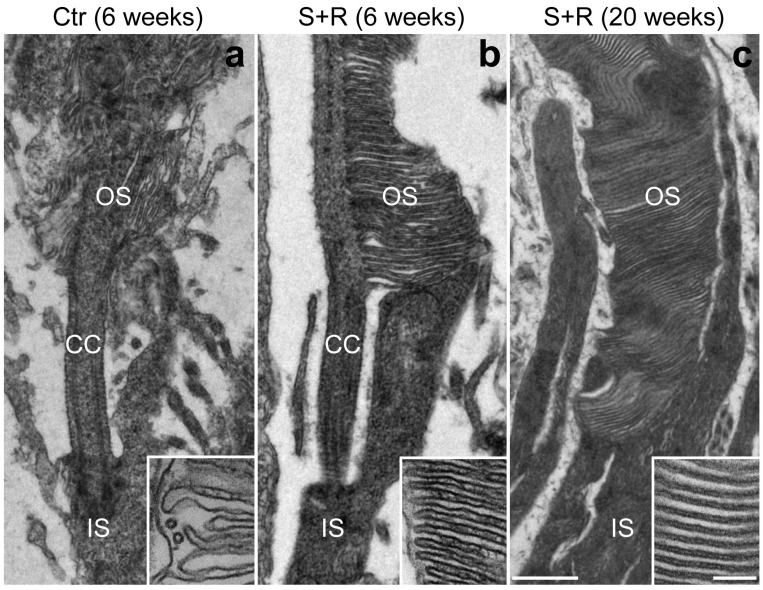

Figure 6.

Photoreceptor morphology rescue following combined suppression and replacement therapy. The right eyes of P5 *P347S* mice were subretinally injected with a mixture of 6.0×10^{8} vp AAV-S and 1.8×10^{10} vp AAV-R (b and c; n=3 and n=1 respectively) while the left eyes were injected with 6.0×10^{8} vp AAV-C (a; n=4). Note that AAV-S and AAV-C co-express EGFP. Six (a and b) and twenty (c) weeks post-injection, eyes were fixed, whole mounted and transduced areas identified by EGFP fluorescence and excised. The excised retinal samples were processed for transmission electron microscopy (TEM). Combined suppression and replacement therapy resulted in the preservation of rod photoreceptor outer segments (OS) with correctly formed membrane disks (b and c). In contrast in control retinas the rod photoreceptor inner segments (IS) attached to truncated OS with disorganized disks. CC: connecting cilium. Scale bars: 500 nm and 100 nm (inserts).